phys. stat. sol. (a) **175**, 345 (1999)

Subject classification: 68.35.Ct; 61.16.Ch; 78.30.Fs; 78.90.+t; S7.12; S7.15

Chemical Contrast Observed at a III–V Heterostructure by Scanning Near-Field Optical Microscopy

A. CRICENTI[1]) (a), R. GENEROSI (a), G. HEROLD (b), P. CHIARADIA (c), P. PERFETTI (a), G. MARGARITONDO (d), J.M. GILLIGAN (e), and N.H. TOLK (e)

(a) Istituto di Stuttura della Materia, CNR, via Fosso del Cavaliere 100, I-00133 Roma, Italy

(b) Vanderbilt University Free-Electron Laser Center, Vanderbilt University, Nashville, Tennessee 37235, USA

(c) Dipartimento di Fisica, Universitá di Roma "Tor Vergata", I-00185 Roma, Italy

(d) Institut de Physique Appliquée, Ecole Polytecnique Fédérale, CH-1015 Lausanne, Switzerland

(e) Department of Physics and Astronomy, Vanderbilt University, Nashville, TN 37235, USA

(Received May 8, 1999)

We observed chemical contrast with subwavelength resolution on a III–V heterostructure by a scanning near-field optical microscope (SNOM) working in the external reflection mode and coupled with a Free Electron Laser (FEL). SNOM reflectivity images revealed features that were not present in the corresponding shear-force (topology) images and are due to localized lateral changes in the optical properties of the sample. The data indicate an optical spatial resolution well below the diffraction limit of $\lambda/2$ with most optical images having better lateral resolution than topographic images.

1. Introduction

The usefulness of scanning near-field optical microscopy (SNOM) for applications such as imaging and analysis of semiconductor devices [1 to 3], microstructural spectroscopy of organic films [4, 5], and biological research [6, 7], has been well documented in the recent literature. We have recently developed an approach based on the combination of spectroscopy with infrared radiation emitted by a free electron laser (FEL) and SNOM [8 to 10] to investigate lateral variations in the bulk optical properties, with lateral resolution well below the diffraction limit. This approach enabled us to measure the local optical properties of a buried PtSi/Si interface [11] and of diamond grains on top of a silicon surface [12] with a lateral resolution between $\lambda/10$ and $\lambda/15$.

The use of FEL radiation makes it possible to illuminate the entire area of large samples thus guaranteeing the homogeneity of the photon excitation. If the reflected signal is collected by a stretched optical fiber with a very small open edge aperture and in near-field conditions, it is possible to perform spatially resolved measurements with lateral resolution well below the diffraction limit. The near-field condition is verified by the shear-force approach [13] that also supplies the local topology at the same time and for the same small area, where we detect the optical signal. With this approach, it is possible to reach a lateral resolution of few tens of nanometers, as demontrated by several tests [14, 15].

[1]) Corresponding author: Tel.: 39-0649934143; Fax: 39-0649934153;
e-mail: antonio@dns.ism.rm.cnr.it

In the present paper, we studied a III–V heterostructure by SNOM in the external reflection mode and coupled with a Free Electron Laser. SNOM reflectivity images revealed features that were not present in the corresponding shear-force (topology) images and are due to localized lateral changes in the optical properties of the sample. While changing the incoming photon energy we have observed chemical contrast for the heterostructure. The data indicate an optical spatial resolution well below the diffraction limit of $\lambda/2$, with most optical images having better lateral resolution than the topographic images.

2. Experiment

Our samples were heterolayers of a III–V semiconductor ($Al_xGa_{1-x}As$) deposited on a different III–V semiconductor (GaAs). The apparatus for controlling the SNOM scanning unit, the data acquisition system and the image processing were described in detail elsewhere [16 to 18]. To detect a shear force signal, a 670 nm single-mode diode laser ($P = 1$ to 4 mW, LaserMax Inc.), equipped with a home-made front lens, producing a minimum spot size of 5 μm, is mounted on an adjustable plate with two spring-loaded stainless steel screws. The laser beam is focused onto the back end of the oscillating fiber used as the scanning probe. The resulting shadow is revealed by a two-sector position sensitive detector placed on the opposite side. The alternating signal is revealed by an ac/dc converter and fed into the electronic feedback loop to keep a constant shear-force signal between fiber and sample while scanning the sample. Shear-force images are taken with a signal corresponding to 70% of the amplitude of free oscillation.

Either a 0.63 μm diode laser or the Vanderbilt Free Electron Laser operating at 2.4 μm (first harmonic, 1.2 μm with frequency doubler) were used to illuminate the sample. Topographical and optical images were taken simultaneously, with either the FEL or the diode laser illuminating the specimen over a broad area and the SNOM probe collecting the locally reflected light. All the images shown here are unfiltered, and only a constant background was performed; brighter areas correspond to higher topography values (or to higher current in the optical image). SNOM (IR-SNOM) probes were fabricated starting from single-mode silica fibers (with outside diameter 125 μm and core approximately 5.5 μm) using a standard micropipette puller.

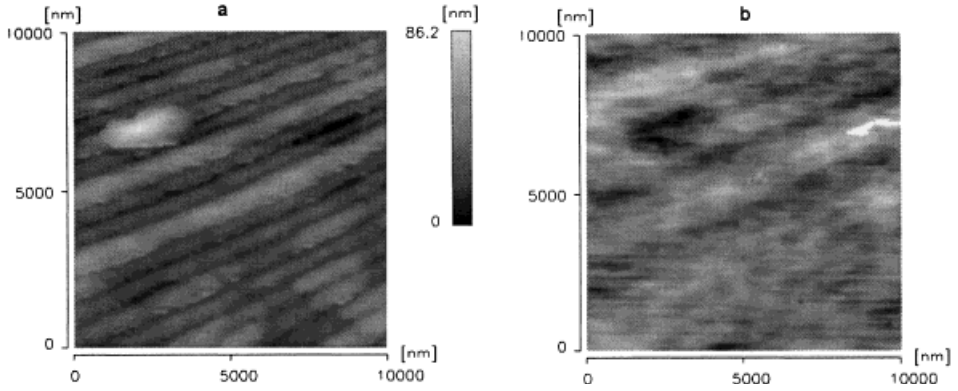

Fig. 1. a) Shear-force SNOM image (10×10 μm^2) of a GaAs/AlGaAs multi quantum well sample. b) Corresponding reflectivity image taken with a photon wavelength of 1.2 μm

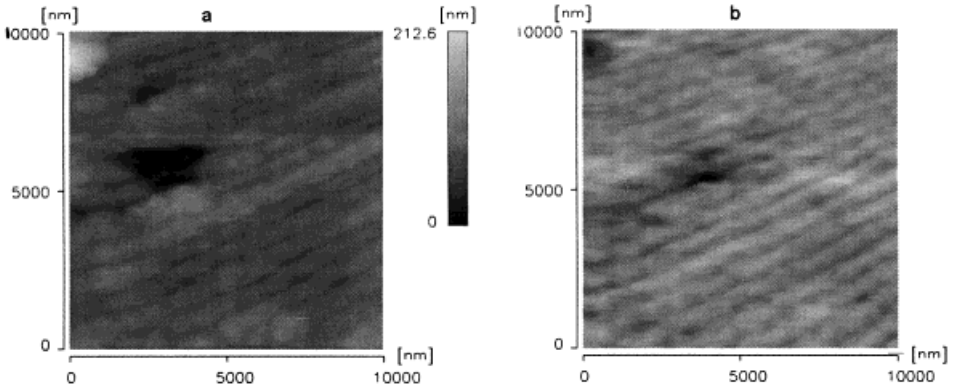

Fig. 2. a) Shear-force SNOM image (10×10 μm^2) of a GaAs/AlGaAs multi quantum well sample. b) Corresponding reflectivity image taken with a photon wavelength of 0.63 μm

3. Experimental Results

Fig. 1a is a 10×10 μm^2 shear-force image taken on a GaAs/Al_xGa_{1-x}As multi quantum well sample: several wells are clearly visible as well as a large defect area, the white spot in the upper left corner. Fig. 1b is the corresponding reflectivity image taken with a photon wavelength of 1.2 μm: a rather weak contrast is observed among the wells whereas the defect area in the upper left corner corresponds to a minimum in the reflectivity. Fig. 2a is a 10×10 μm^2 shear force image taken on another zone of the sample: several wells are again here clearly visible as well as a valley (dark spot) and a bump (white spot) in the upper left corner. Fig. 2b is the corresponding reflectivity image taken with a photon wavelength of 0.63 μm: in this case a strong contrast is observed among the wells while the valley and the bump in the upper left corner correspond to minima in the reflectivity. The different quantum well contrast observed in the

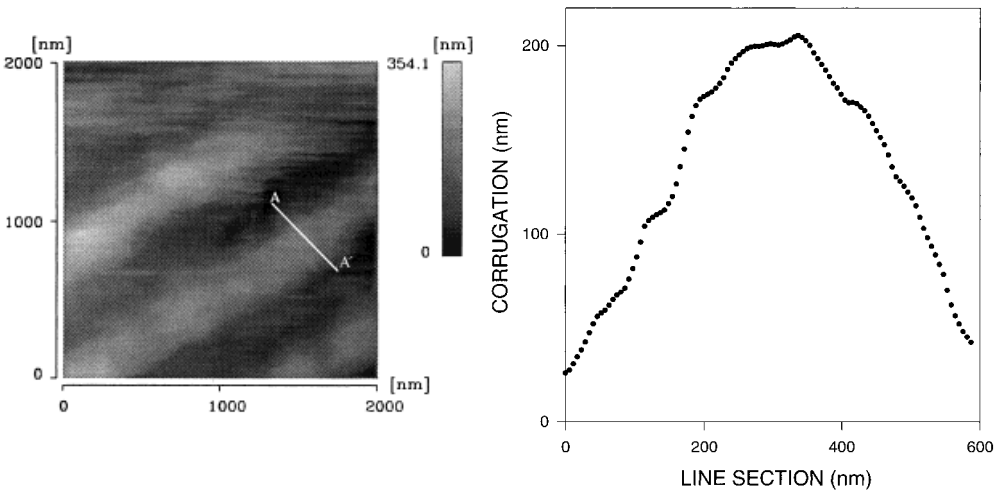

Fig. 3. Left part: shear-force SNOM image (2×2 μm^2) of a GaAs/AlGaAs multi quantum well sample. Right part: intensity profile along the A–A′ line

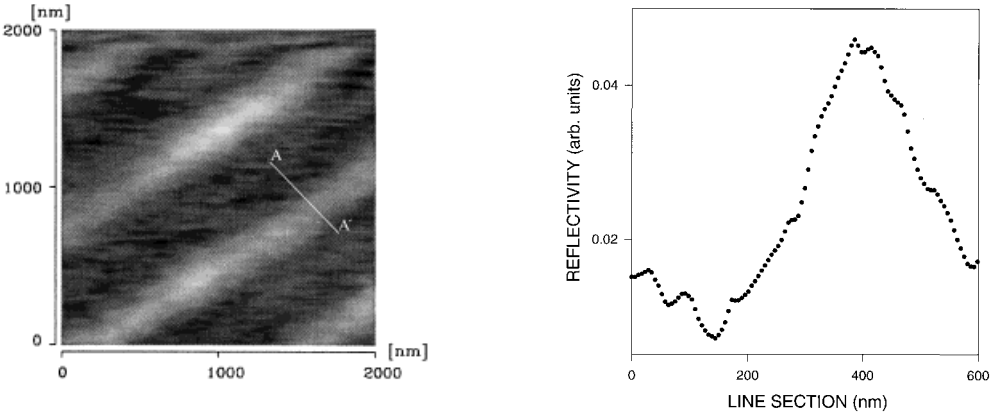

Fig. 4. Left part: reflectivity image corresponding to the same zone as Fig. 3a taken with a photon wavelength of 0.63 μm. Right part: intensity profile along the A–A′ line

two reflectivity images can be explained by the different optical properties of the two III–V materials at these two wavelengths. In fact, at 1.2 μm both materials are transparent and do not contribute to the reflectivity signal; the reflectivity contributions are due to scattered light and to the defect area. At 0.63 μm, the contrast between the two semiconductors is due to the fact that GaAs is strongly absorbing while the AlGaAs absorption edge is very close and then the absorption is quite weak.

Fig. 3a is a 2×2 μm^2 shear force image taken on a GaAs/$Al_xGa_{1-x}As$ multi quantum wells and Fig. 3b is the intensity profile along the A–A′ line. The profile shows that the quantum wells have a 600 nm width and 170 nm height. Fig. 4a and b show the corresponding reflectivity image and an intensity profile along the A–A′ line for a photon wavelength of 0.63 μm. The same features are revealed by both images even though the optical image exibits a narrower well width, probably due to the fact that the hole at the tip apex is smaller than the curvature radius of the optical fiber end. For these samples, most of the images taken in the optical mode have better lateral resolution than the topographic data. This is a crucial point in determining whether the optical image is a real near-field effect or it is a z-motion artifact image [19]. The present images, corroborated by many others, demonstrate we obtained a lateral resolution between $\lambda/6$ and $\lambda/10$, well below the classical diffraction limit of $\lambda/2$ and, therefore, that we achieved SNOM conditions.

References

[1] R.M. CRAMER, L.J. BALK, R. CHIN, R. BOYLAN, S.B. KÄMMER, F.J. REINEKE, and M. UTLAUT, Proc. 22nd Internat. Symp. Testing and Failure Analysis, Los Angeles (CA) November 1996 (p. 19).
[2] J.P. FILLARD, DRIP '95, Inst. Phys. Conf. Ser. **49**, 195 (1996).
[3] B.B. GOLDBERG, H.F. GHAEMI, M.S. ÜNLÜ, and W.D. HERZOG, Mater. Res. Soc. Symp. Proc. **406**, 171 (1996).
[4] L.A. NAGAHAR, H. YANAGI, and H. TOKUMOTO, Nanotechnology **8**, A50 (1997).
[5] E. BETZIG and R.J. CHICHESTER, Science **262**, 1422 (1993).
[6] H. HEINZELMANN and D.W. POHL, Appl. Phys. A **59**, 89 (1994).
[7] W. JIA and L. DACHENG, Proc. SPIE **2535**, 115 (1996).
[8] D.W. POHL, W. DENK, and M. LANZ, Appl. Phys. Lett. **44**, 651 (1984).

[9] E. Betzig, J.K. Trautman, T.D. Harris, J.S. Weiner, and R.L. Kostelak, Science **251**, 1468 (1991).
[10] D. Courjon and C. Bainier, Rep. Progr. Phys. **57**, 989 (1994).
[11] A. Cricenti, R. Generosi, P. Perfetti, J.M. Gilligan, N.H. Tolk, C. Coluzza, and G. Margaritondo, Appl. Phys. Lett. **73**, 151 (1998).
[12] A. Cricenti, R. Generosi, C. Barchesi, M. Luce, M. Rinaldi, C. Coluzza, P. Perfetti, G. Margaritondo, D. T. Schaafsma, I. D. Aggarwal, J. M. Gilligan, and N. H. Tolk, phys. stat. sol. (a) **170**, 241 (1998).
[13] D.W. Pohl and D. Courjon (Eds.), Near Field Optics, NATO ASI Series, Vol. 262, Kluwer Academic Publ., Dordrecht 1992.
[14] J. Almeida et al., Appl. Phys. Lett. **69**, 2361 (1996).
[15] C. Coluzza, J. Almeida, T. dell'Orto, O. Bergossi, M. Spajer, S. Davy, D. Courjon, A. Cricenti, R. Generosi, P. Perfetti, and G. Faini, Proc. SPIE **2782**, 591 (1997).
[16] A. Cricenti, R. Generosi, C. Barchesi, M. Luce, and M. Rinaldi, Rev. Sci. Instrum. **69**, 3240 (1998).
[17] A. Cricenti and R. Generosi, Rev. Sci. Instrum. **66**, 2843 (1995).
[18] C. Barchesi, A. Cricenti, R. Generosi, C. Giammichele, M. Luce, and M. Rinaldi, Rev. Sci. Instrum. **68**, 3799 (1997).
[19] B. Hecht, H. Bielefeldt, Y. Inouye, D.W. Pohl, and L. Novotny, J. Appl. Phys. **81**, 2492 (1997).